Hindawi Publishing Corporation
International Journal of Electrochemistry
Volume 2012, Article ID 410846, 8 pages
doi:10.1155/2012/410846

Research Article

Improvement of Amperometric Biosensor Performance for H_2O_2 Detection based on Bimetallic PtM (M = Ru, Au, and Ir) Nanoparticles

Yuan Zhang,[1] Metini Janyasupab,[2] Chen-Wei Liu,[3] Po-Yuan Lin,[4] Kuan-Wen Wang,[3] Jiaqiang Xu,[1] and Chung-Chiun Liu[2]

[1] *Department of Chemistry, Shanghai University, Shanghai 200444, China*
[2] *Department of Chemical Engineering, Case Western Reserve University, Cleveland, OH 44106, USA*
[3] *Institute of Materials Science and Engineering, National Central University, Chung-Li 320, Taiwan*
[4] *Department of Material Science and Engineering, Case Western Reserve University, Cleveland, OH 44106, USA*

Correspondence should be addressed to Yuan Zhang, yxz412@case.edu

Received 13 September 2011; Revised 26 October 2011; Accepted 28 October 2011

Academic Editor: Ulku Anik

Novel bimetallic nanoparticles have been synthesized via rapid microwave irradiation, leading to an improved sensitivity and a highly anti-interference property for amperometric biosensor in H_2O_2 detection. The material characterizations were performed by TEM, XRD, and EDX, which show the bimetallic formation of Pt-based catalysts and well-dispersed nanoparticles of 2–5 nm. The sensitivities for the detection of H_2O_2 of PtRu, PtAu, and PtIr as the biosensor working electrode catalysts are 539.01 (R^2 = 0.99), 415.46 (R^2 = 0.99), and 404.52 (R^2 = 0.97) $\mu A \cdot mM^{-1} \cdot cm^{-2}$, respectively, nearly twice higher than the pure Pt catalyst (221.77 $\mu A \cdot mM^{-1} \cdot cm^{-2}$, R^2 = 0.98), at a low applied potential of +0.25 V versus Ag/AgCl. Furthermore, Pt-Ru and Pt-Ir show a highly sensitive response and a promising anti-interference capability to ascorbic acid, a major interferent, by reducing the interferent current as low as 7-8% significantly lower than that of Pt (30% change). The enhancement of both sensitivity and selectivity in the bimetallic catalysts can be found practical applications in biosensing.

1. Introduction

Platinum (Pt), a well-known and traditional heterogeneous catalyst, plays an important role in thermo, photo and electrocatalysis [1–3], and it is widely used in advanced optical, electronic, magnetic, and sensing devices [4–7]. The reactivity and selectivity of heterogeneous catalysts usually depend on their surface active sites, and therefore the synthesis of nanoparticles with controlled shapes and sizes is critical for tuning the surface active sites and important for improving their applications [8–10]. Well-dispersed Pt nanoparticles with different morphologies, such as polyhedral, truncated cubic, and cubic nanocrystals have been controllably synthesized and applied to biosensors [11–13]. In selected enzymatic reactions, the substrate (analyte) is oxidized, yielding intermediates (e.g., adsorbed CO and OH species), which tend to cover the active sites on the Pt catalysis surface [14, 15]. Consequently, the efficiency of the catalyst becomes limited, resulting in low sensibility and poor selectivity for biosensing applications.

By using Pt with adatoms on the surface or Pt-containing bimetallic nanocrystals, the catalysts resistance to poison can be enhanced [16–18]. Xiao et al. synthesized AuPt alloy nanoparticles that deposited ionic liquid-chitosan composite film and used nonenzymatic H_2O_2 detection [19]. The results reflected a remarkable synergistic effect, and the presence of Au could reduce the strength of Pt–OH formation providing needed adsorption sites for –OH species [19]. Furthermore, not only the resistance to poison can be improved by adopting bimetallic materials, the sensitivity and stability of biosensors were also enhanced. Muraviev et al. synthesized polymer-stabilized monometallic Pt (Pt-PSMNPs) and bimetallic Pt/Cu core-shell nanoparticles (Pt/Cu-PSMNPs) as sensing elements to detect H_2O_2 [20].

The results showed that the electrocatalytic activity of Pt/Cu-PSMNPs was far higher than that of monometallic Pt-PSMNPs [20]. Rajkumar et al. fabricated rhodium-palladium (Rh-Pd) particles modified, on glassy carbon electrode (GCE) and successfully used it for detecting H_2O_2 in a real samples (10–340 μM), which was stable for 2 days, and gradual decreases occurred in the reduction and oxidation peak potentials [21].

Many measurements of biosensors were conducted for the detection of enzymatically generated H_2O_2 based on the enzymatic reaction. For example, the detection of the bile acids was based on the enzymatically formed nicotinamide adenine dinucleotide (NADH). By using an additional enzyme, NADH could be converted to NAD^+ and generates H_2O_2 [22]. Higher concentrations of the bile acids would result in greater concentrations of enzymatically produced H_2O_2, which can be used to quantify bile acids in the testing medium. And there are also many other biomarkers, such as adenosine deaminase, glucose, pyruvate, lactate, and cholesterol, that are able to generate H_2O_2 in corresponding enzymatic reaction [23–26]. In this study, we describe the synthesis and characterization of different Pt-containing bimetallic nanoparticles and demonstrate their electrocatalytic properties by catalytic oxidation of H_2O_2. Consequently, the electrochemical oxidation current of H_2O_2 can then be used to quantify the analyte. The sensitivity of the Pt-based bimetallic nanocatalysts to the oxidation of H_2O_2 was investigated, and the interference from ascorbic acid (AA), a potentially major interference species, was also evaluated.

2. Experimental

2.1. Rapid Synthesis of Pure Pt and Bimetallic Nanoparticles. Pure Pt and Pt-based bimetallic nanoparticles were prepared by microwave heating of a highly dielectric solvent, ethylene glycol, (EG, Fisher, AR) solutions of Pt, and the other metal precursor salts. As a typical process for the synthesis of Pt nanoparticles, 0.75 mL of an aqueous solution of 0.05 M $K_2PtCl_6 \cdot 6H_2O$ (Aldrich, ACS Reagent) was mixed with 25 mL of EG and 0.75 mL of 0.4 M KOH in a 300 mL beaker. The beaker was then placed in the center of a household microwave oven (Panasonic, 1250 W) and heated for 36 s. For the preparation of PtRu and PtIr bimetallic nanoparticles, the starting mixture contained 25 mL EG, 0.75 mL 0.05 M $K_2PtCl_6 \cdot 6H_2O$ aqueous solution, 0.75 mL 0.05 M $RuCl_3$ (Aldrich, ACS Reagent) or 0.05 M $IrCl_3$ (Aldrich, ACS Reagent) aqueous solution, respectively, and 0.75 mL 0.04 M KOH solution. In the preparation of PtAu nanoparticles, the concentration of Pt and Au precursors was reduced to 0.025 M, the other reagents were maintained the same. The resulting pure Pt and bimetallic solutions (pure Pt: 11.60 mL, PtRu: 10.97 mL, PtIr: 5.96 mL, and PtAu: 11.76 mL) were mixed with 16 mg of carbon powder (Vulcan XC 72R, Cabot, USA) by ultrasound for 2 hours, respectively. These Pt-based bimetallic nanoparticles were mixed with the carbon powder, producing a printable ink to be evaluated and used for electrochemical characterization. The nanoparticle metal and carbon mixtures were washed with acetone and ethanol in sequence three or four times. After centrifuging and drying at 60°C under vacuum for 12 h, the mixed electrocatalysts were obtained and were ready to be used.

2.2. Characterization and Measurements. The morphology, size, and compositions of pure Pt and bimetallic nanoparticles were characterized by transmission electron microscopy (TEM, Techai F30, using an accelerating voltage of 300 kV) and energy-dispersive X-ray spectroscopy (EDX). The crystal phase of as-synthesized products was identified by powder X-ray diffraction (XRD) analysis (CuK_α, $\lambda = 1.54056$ Å, Scintag X-1, USA), and the XRD data were collected at a scanning rate of 0.02° s^{-1} for 2θ in a range from 10° to 80°.

2.3. Electrochemical Characterization. Typically, 8 mg of the electrocatalysts was dispersed in ethanol (200 μL) and Nafion solution (100 μL, 5% wt.) in an ultrasonic bath for 30 minutes. Eight microliters of the mixture (the ink) was deposited onto a glassy carbon working electrode (0.5 cm in diameter, AFE2M050GC, Pine Instrument) and dried in ambient air for 3 minutes. The working electrode was operated at the rotational speed of 900 rpm with Ag/AgCl reference and Pt mesh counter electrode (1 cm × 1 cm). The sensing characteristics of all the electrocatalysts were investigated with various concentrations of H_2O_2 in a phosphate buffer solution (PBS) of pH 7.4. Cyclic voltammetric and amperometric measurements (Electrochemical Workstation CHI 660A) were performed to determine the electrochemical response of H_2O_2.

3. Results and Discussion

3.1. Structure and Morphology. The morphology and size of pure Pt and bimetallic nanoparticles were characterized by TEM (shown in Figure 1). The as-prepared particles are well dispersed and substantially uniform in size. By controlling the time of microwave irradiation and the concentration of metal precursors, different metals in the same size range can be obtained. When the Pt precursor mixed with KOH and EG solution was placed into the microwave and heated for 36 s, Pt nanoparticles with diameter about 3–5 nm were obtained (Figure 1(a)). Upon microwave irradiation for 28 s, bimetallic PtRu nanoparticles with a diameter of about 2-3 nm were formed (Figure 1(b)). Decreasing the concentration of Pt and Au precursor to 0.025 M yielded nanoparticles with a diameter of about 2–4 nm (Figure 1(c)). The particles size of PtIr is about 2-3 nm, which was obtained by heating the precursor solution for 20 s (Figure 1(d)).

Figure 2 is the EDX analysis of pure Pt and bimetallic nanoparticles. In the spectra of PtRu, PtIr, and PtAu, the peaks of Pt, Ru, Ir, and Au confirm the coexistence of two metals in each sample, respectively. Cu and C peaks presented in the samples come from the copper grid used to support the samples, and Fe, Co peaks are caused from the column in TEM instrument.

XRD measurements were used to identify the prepared pure Pt and bimetallic nanoparticles. It can be seen from Figure 3 that all the peaks in the XRD pattern of pure Pt

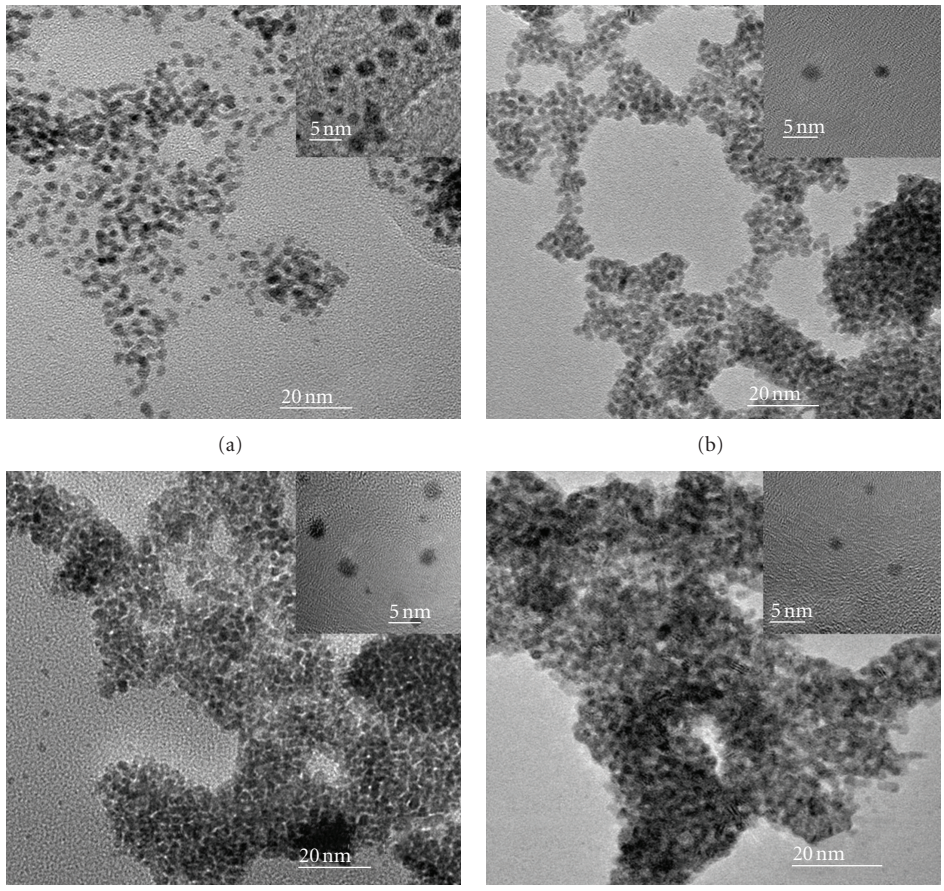

Figure 1: The TEM images of pure Pt (a) and bimetallic PtRu (b), PtAu (c) and PtIr (d) nanoparticles.

were well indexed to Pt (JCPDS No. 87-0640, $a = b = c = 0.3923$ nm) with high crystallization. As the bimetallic nanoparticles are formed, all the peaks in the XRD patterns of PtRu and PtIr are shifted slightly to larger 2θ values (right-shift) with respect to the pure Pt, indicating the decreased d-spacings and contraction of the lattice constant, due to the incorporation of increasing amounts of the smaller metal atoms into the Pt fcc lattice [27]. On the other hand, the XRD peaks of PtAu are shifted slightly to smaller 2θ values (left-shift) pattern, implying that the incorporation of larger Au atoms into the Pt fcc lattice. No Pt or other metal peaks appear, indicating that bimetallic nanostructures or alloys were formed.

3.2. Biosensing Characterization

3.2.1. Amperometric Determination of Pure H_2O_2. Because many enzymatic reactions that are related to the key enzyme in a biological system generate H_2O_2 as a by-product, therefore, the detection of H_2O_2 is important to biosensing. The performance biosensing of the pure Pt and the bimetallic catalysts was assessed by electrocatalytic oxidation of H_2O_2. First, cyclic voltammogram was carried out at an ambient temperature (22.0°C) in the presence and absence of 0.25 mM H_2O_2 in a 75 mL test medium. Figure 4 shows the cyclic voltammograms of pure Pt, PtRu, PtAu, and PtIr from −0.2 to +0.6 V versus the Ag/AgCl reference electrode, at 50 mV/s scan rate. While the oxidation of H_2O_2 for the pure Pt catalyst starts at +0.23 V, all bimetallic catalysts begin even before this potential. For instance, the oxidation of H_2O_2 was started from 0.20, 0.20, and 0.15 V versus Ag/AgCl in the voltammograms of bimetallic PtRu, PtAu, and PtIr, respectively, and these results clearly demonstrated the enhanced electrocatalytic ability of the bimetallic nanoparticles toward the detection of H_2O_2 at relatively low electrochemical potentials. The performance of bimetallic nanoparticles in this work is compared with other catalysts as shown in Table 1, suggesting superior performance in terms of onset catalytic potential. The selection of the applied potential to oxidize H_2O_2 could be based on the results as shown in Figure 4, and also the relatively higher potential of pure Pt toward the detection of H_2O_2 should be considered to oxidize other coexisting electroactive species. Hence, an applied potential of +0.25 V versus the Ag/AgCl reference electrode was then chosen in order to minimize the potential interference from the oxidation of the other species in the test medium.

The amperometric detection of different concentration of H_2O_2 was then tested. Different concentrations of H_2O_2 solution ranging from 0.25 to 3.25 mM were prepared,

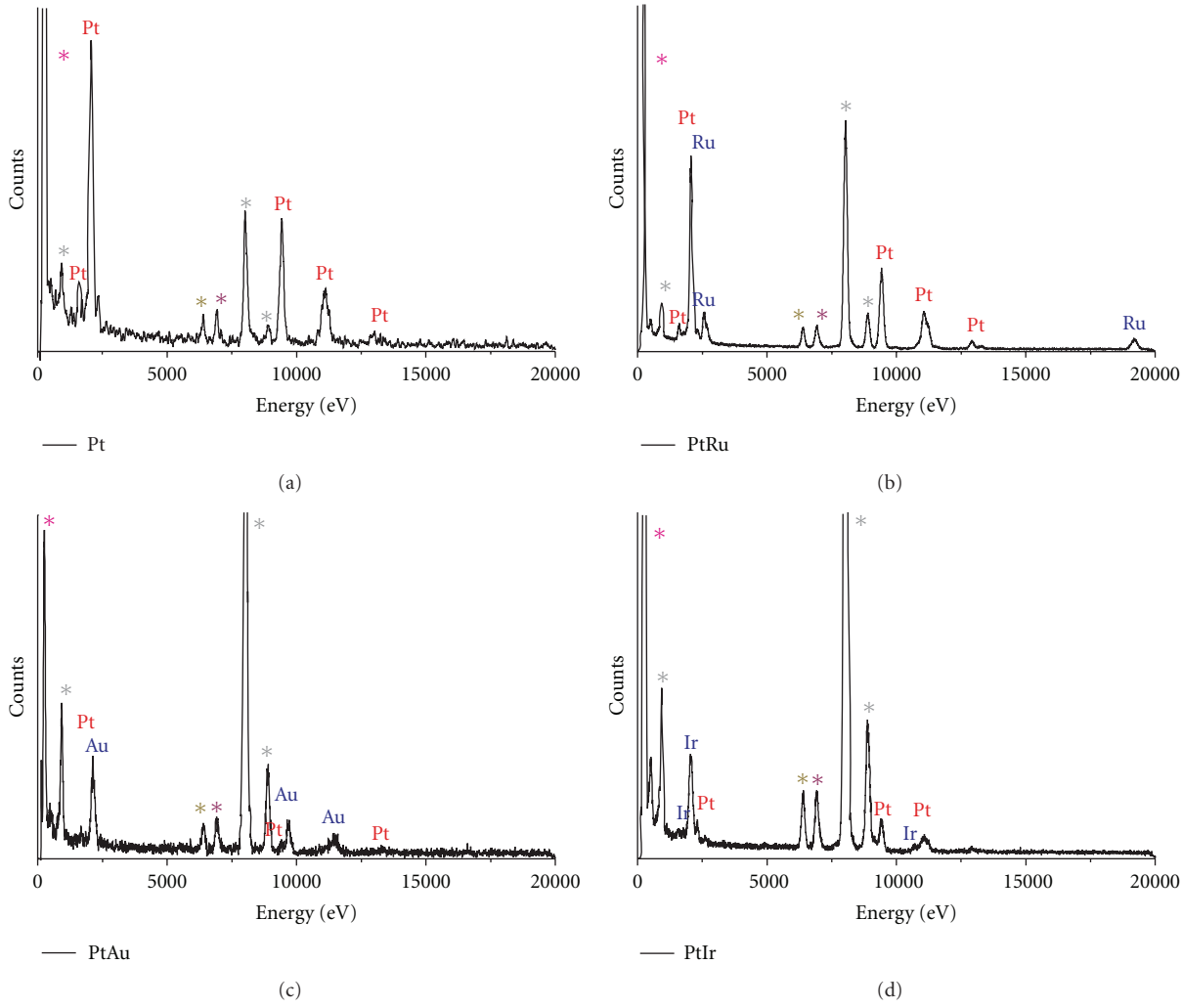

Figure 2: EDX spectra of pure Pt (a) and bimetallic PtRu (b), PtAu (c) and PtIr (d) nanoparticle. (TEM instrument, carbon, and copper grid spectra corresponding to olive green asterisk: Fe, violet asterisk: Co, pink asterisk: C, and gray asterisk: Cu).

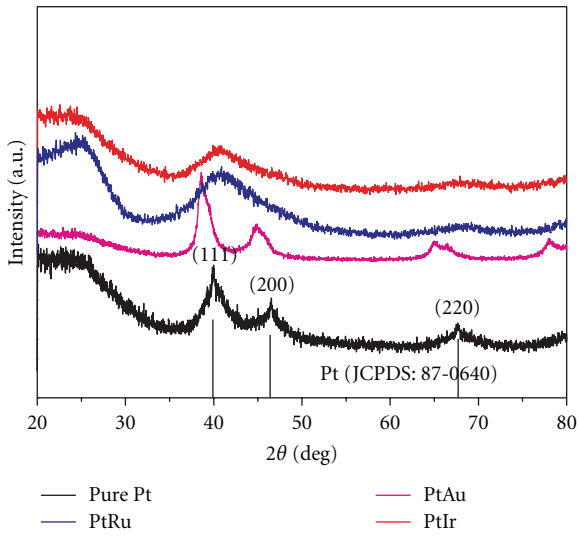

Figure 3: XRD spectra of pure Pt and bimetallic nanoparticles.

and the amperometric measurement technique was used to record the change in the current as a function of time. The applied potential was +0.25 V versus the Ag/AgCl reference electrode. Figure 5 shows the real time responses of different metal to different concentration of H_2O_2. The current increase was observed with multiple injections of H_2O_2. All the four metals demonstrated a stepwise increase in current corresponding to an increase in the supplemental concentration of H_2O_2. Also, we find that the current increase of pure Pt is much lower than bimetallic PtRu, PtAu, and PtIr nanoparticles, especially at higher H_2O_2 concentration.

Figure 6 shows the current concentration plot of bimetallic compounds as compared to the pure Pt to detect H_2O_2 from 0.25 mM to 3.25 mM. In particular, the sensitivities of PtRu, PtAu, and PtIr are estimated to be 539.01, 415.46, and 404.52 $\mu A \cdot mM^{-1} \cdot cm^{-2}$, respectively, twice as high as that of the pure Pt (221.77 $\mu A \cdot mM^{-1} \cdot cm^{-2}$). Not only did both PtRu and PtIr have a comparable sensitivity, but also showed a high degree of repeatability as indicated by the

Table 1: Comparison of the performance of various H_2O_2 sensors based on electrochemical measurement.

Catalyst	Sensitivity ($\mu A \cdot mM^{-1} \cdot cm^{-2}$)	% RSD	LOD (μM)	Applied potential versus Ag/AgCl (V)	References
Pt NPs	221.77	10.5	3.3	+0.25	This work
PtRu NPs	539.01	0.5	1.7	+0.25	This work
PtAu NPs	415.46	9.1	2.0	+0.25	This work
PtIr NPs	405.52	2.0	0.8	+0.25	This work
Hb/GNPs/Hb/MWNT	205.41	3.5	0.08	−0.3	[28]
Ag NPs/GO	13.93	3.9	1.9	−0.3	[29]
Pt/TiO_2/CNT	0.85	5.5	4	+0.3	[30]
CNT/Pt NPs	$1.8 * 10^3$	3.5	1.2	+0.55	[31]
MP-Pt-ME	$2.8 * 10^3$	no	4.5	+0.6	[32]

NPs: nanoparticles, Hb: hemoglobin, GNPs: gold nanoparticles, MWNT: multiwall carbon nanotubes, GO: graphene oxide, MP: mesoporous, ME: microelectrode, CNT: carbon nanotube RSD: relative standard deviation, LOD: limit of detection, RSD of Hb/CNT/Au NPs: $n = 9$ (0.1 mM H_2O_2), RSD of Ag NPs/GO: $n = 5$ (1 mM H_2O_2), RSD of GC/CNT/Pt NPs: $n = 8$ (1 mM), RSD of Pt/TiO_2/CNT: $n = 8$ (0.2 mM H_2O_2), negative applied potential: reduction, and positive applied potential: oxidation.

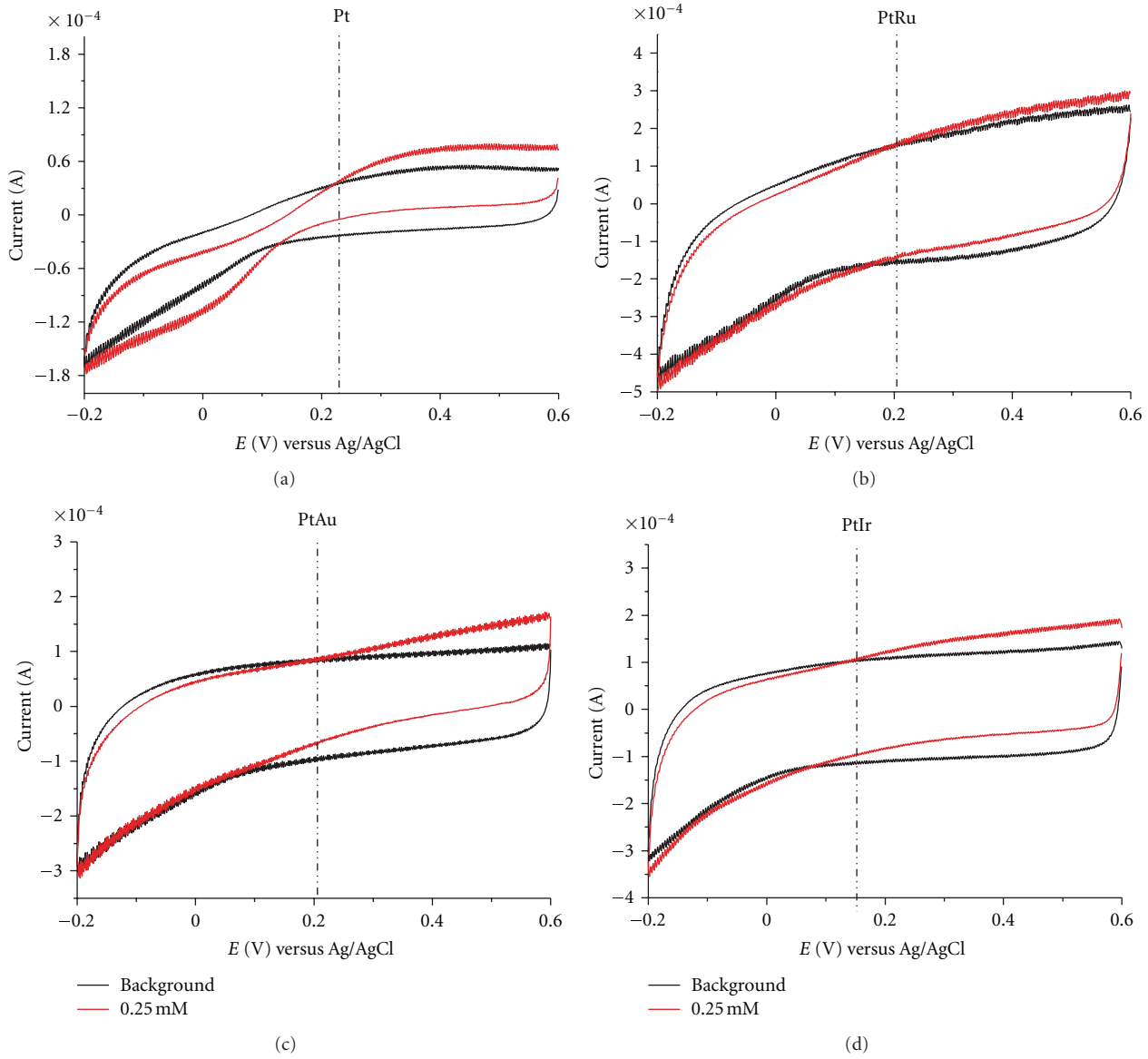

Figure 4: Cyclic voltammetric responses of different metallic catalysts at 0.25 mM H_2O_2 in PBS (pH = 7.4), at 50 mV/s scan rate.

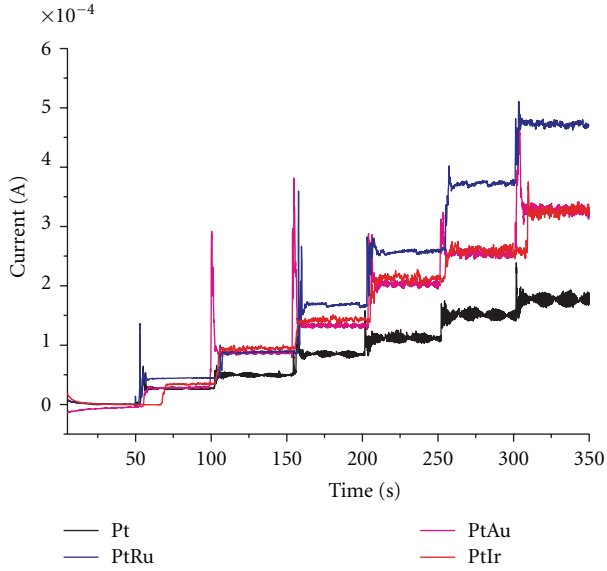

Figure 5: Typical amperometric response of different metals to different concentrations of H_2O_2 (0.25 mM, 0.5 mM, 0.75 mM, 1.25 mM, 2.25 mM, and 3.25 mM).

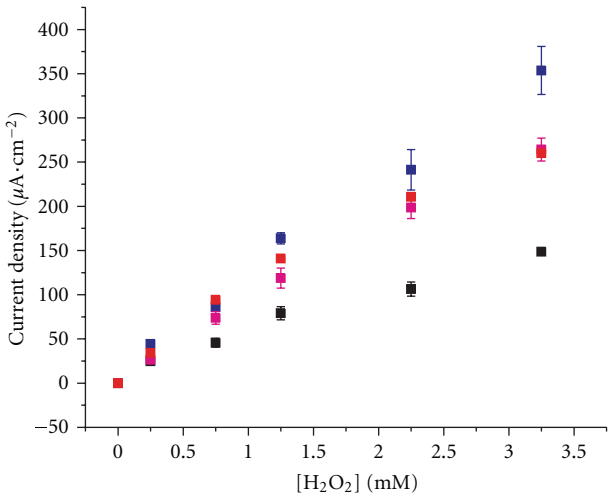

Metal	Sensitivity ($\mu A \cdot mM^{-1} \cdot cm^{-2}$)	R^2
Pt	221.77	0.98
Pt-Ru	539.01	0.99
Pt-Au	415.46	0.99
Pt-Ir	404.52	0.97

Figure 6: Current concentration of H_2O_2 calibration plots at +0.25 V versus Ag/AgCl.

relative standard deviation (RSD). Six different PtRu and PtIr electrodes, fabricated using the same procedures, yield the results of high reproducibility with RSD of 0.5% and 2.0% towards the response of 0.25 Mm H_2O_2, respectively. The detection limit of PtRu, PtAu, and PtIr are estimated to be 2.0, 1.7, and 0.8 μM at a signal-to-ratio of 3, which is lower than 3.3 μM on pure Pt nanoparticles. Based on this property, both PtRu and PtIr show a better accuracy in measurement and wider linear range of detection. In

Table 2: Comparison of oxidation current change at 0.5 mM H_2O_2 detection with a presence of AA.

Metal compound	Current density ($\mu A \cdot mM^{-1} \cdot cm^{-2}$)		Percentage change
	Only 0.5 mM H_2O_2	0.5 mM H_2O_2+ 5 mg/L AA	
Pt	11.70	15.14	29.40
Pt-Au	114.19	115.86	1.46
Pt-Ir	115.00	123.73	7.59
Pt-Ru	105.54	97.20	7.90

term of linearity, R^2 values of all catalysts indicate a good linear relationship between oxidation current and H_2O_2 concentration. Among the bimetals, PtRu outperformed the other two metal compounds with the highest sensitivity with an excellent R^2 value = 0.99, providing a desirable characteristics to detect pure H_2O_2 at this low applied potential. In Table 1, our study shows that even without the integration of high surface area supporting materials (e.g., GO, CNT), the incorporation of bimetals allows the catalyst operating at lower applied potential and maintaining high electrocatalytic activity. Studies [31, 32] by Hrapovic et al. and Evans et al. report the higher sensitivity than this work. However, the applied potentials (+0.55 and +0.6 V) are also significantly higher, which can easily oxidize ascorbic acid, uric acid, dopamine, and other species. Furthermore, 100% loading of catalysts is used in those studies [31, 32], and much less amount of catalyst (20%) is used in this work.

3.2.2. Ascorbic Acid Interference. Further investigation of interference toward H_2O_2 detection was also carried out for biosensing. It has been known that ascorbic (AA) is one of the chemical species in physiological fluid and is commonly oxidized at +0.3 V versus Ag/AgCl. Therefore, in many biosensing applications, AA interferes the sensor performance. As shown in Figure 7, the head-to-head comparison between pure H_2O_2 and mixture of H_2O_2 with high concentration AA (5 mg/L) for each catalyst was presented. The oxidation current at 0.5, 1.0, and 1.5 mM H_2O_2 of the pure Pt shows the effect of AA at +0.3 V as shown by the red color data points. All three bimetallic compounds exhibit an improved selectivity. Especially for the PtIr, the difference in both currents resulted by the pure H_2O_2 and the mixture is nearly negligible for the detection below 1 mM of H_2O_2. At 0.5 mM H_2O_2 with 5 mg/L AA, only 7-8% of oxidation current change will occur by using PtRu and PtIr. A minute interference effect by the ascorbic acid was found to be only 1-2% for PtAu catalyst whose linearity was poorer than the other bimetallic catalysts in this study. By comparison, the single Pt catalyst shows approximately 30% of interference by the ascorbic acid oxidation in H_2O_2 detection as summarized in Table 2. In addition to highly selective property, at +0.3 V, PtRu and PtIr have the sensitivity value of 1236.4 and 1359.7 $\mu A \cdot mM^{-1} \cdot cm^{-2}$, $R^2 = 0.99$, respectively, approximately one order higher than the pure Pt (136.1 $\mu A \cdot mM^{-1} \cdot cm^{-2}$, $R^2 = 0.99$). Hence, both PtRu and PtIr nanoparticles suggest an excellent sensitive and

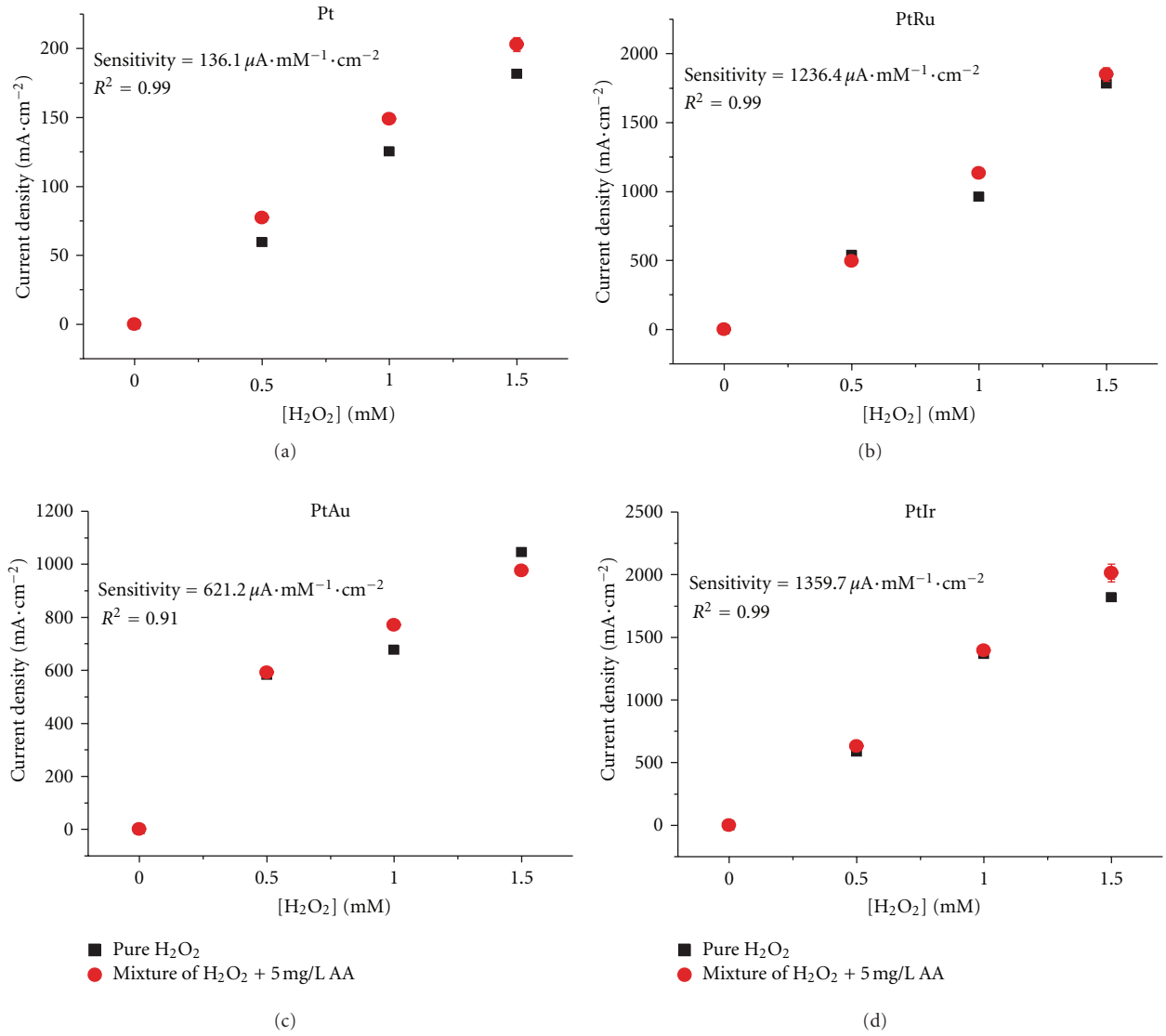

Figure 7: Effect of 5 mg/L AA to H_2O_2 detection at +0.3 V versus Ag/AgCl.

highly capable of anti-interference catalyst, which is superior to the pure Pt. Both bimetallic catalysts can minimize the AA interference and provide better biosensing performance.

4. Conclusions

Bimetallic Pt-Ru, Pt-Au, and Pt-Ir nanoparticle catalysts was successfully synthesized via rapid microwave irradiation with EG and KOH. The structure and morphology was illustrated by TEM images with the average particle size less than 5 nm in diameter. The elemental composition and existing of bimetallic interaction were also confirmed by EDX and shift of XRD peaks, respectively. Furthermore, electrocatalytic properties of bimetals, particularly for PtRu and PtIr show superior performance in both sensitivity and selectivity than the pure Pt at a low applied potential, providing an anti-interference catalyst platform for future biological applications.

Acknowledgments

Financial supports provided by China Scholarship Council Postgraduate Scholarship Program, Royal Thai Government Scholar Fellowship, Taiwan National Central University Fellowship, Delta Environmental and Education Foundation, and the NSF Grant no. 1000768 are gratefully acknowledged.

References

[1] K. Nakano, E. Obuchi, and M. Nanri, "Thermo-photocatalytic decomposition of acetaldehyde over Pt-TiO_2/SiO_2," *Chemical Engineering Research and Design*, vol. 82, no. 2, pp. 297–301, 2004.

[2] Y. Xu and X. Lin, "Selectively attaching Pt-nano-clusters to the open ends and defect sites on carbon nanotubes for electrochemical catalysis," *Electrochimica Acta*, vol. 52, no. 16, pp. 5140–5149, 2007.

[3] I. Yasumori and K. Hirabayashi, "Homogeneous catalysis by Pt(II)-Sn(II) chloride complex. Part 1.—Kinetics and mechanisms of the hydrogenations of acetylene and ethylene," *Transactions of the Faraday Society*, vol. 67, pp. 3283–3296, 1971.

[4] A. Ebbing, O. Hellwig, L. Agudo, G. Eggeler, and O. Petracic, "Tuning the magnetic properties of Co nanoparticles by Pt capping," *Physical Review B*, vol. 84, no. 1, article 012405, 2011.

[5] T. Bak, J. Nowotny, M. Rekas, and C. C. Sorrell, "Photo-electrochemical properties of the TiO_2-Pt system in aqueous solutions," *International Journal of Hydrogen Energy*, vol. 27, no. 1, pp. 19–26, 2002.

[6] L. Mao, R. Yuan, Y. Chai, Y. Zhuo, and W. Jiang, "Potential controlling highly-efficient catalysis of wheat-like silver particles for electrochemiluminescence immunosensor labeled by nano-Pt@Ru and multi-sites biotin/streptavidin affinity," *Analyst*, vol. 136, no. 7, pp. 1450–1455, 2011.

[7] A. Wang, X. Ye, P. He, and Y. Fang, "A new technique for chemical deposition of Pt nanoparticles and its applications on biosensor design," *Electroanalysis*, vol. 19, no. 15, pp. 1603–1608, 2007.

[8] C. Wang, H. Daimon, T. Onodera, T. Koda, and S. Sun, "A general approach to the size-and shape-controlled synthesis of platinum nanoparticles and their catalytic reduction of oxygen," *Angewandte Chemie*, vol. 47, no. 19, pp. 3588–3591, 2008.

[9] L. C. Gontard, L. Y. Chang, C. J. D. Hetherington, A. I. Kirkland, D. Ozkaya, and R. E. Dunin-Borkowski, "Aberration-corrected imaging of active sites on industrial catalyst nanoparticles," *Angewandte Chemie*, vol. 46, no. 20, pp. 3683–3685, 2007.

[10] H. Song, F. Kim, S. Connor, G. A. Somorjai, and P. Yang, "Pt nanocrystals: shape control and Langmuir-Blodgett monolayer formation," *Journal of Physical Chemistry B*, vol. 109, no. 1, pp. 188–193, 2006.

[11] J. S. Ye, A. Ottova, H. T. Tien, and F. S. Sheu, "Nanostructured platinum-lipid bilayer composite as biosensor," *Bioelectrochemistry*, vol. 59, no. 1-2, pp. 65–72, 2003.

[12] Z. Chu, Y. Zhang, X. Dong, W. Jin, N. Xu, and B. Tieke, "Template-free growth of regular nano-structured Prussian blue on a platinum surface and its application in biosensors with high sensitivity," *Journal of Materials Chemistry*, vol. 20, no. 36, pp. 7815–7820, 2010.

[13] S. Wang, L. Lu, and X. Lin, "A selective voltammetric method for uric acid detection at a glassy carbon electrode modified with electrodeposited film containing DNA and Pt-Fe(III) nanocomposites," *Electroanalysis*, vol. 16, no. 20, pp. 1734–1738, 2004.

[14] C. Fu, H. Zhou, D. Xie et al., "Electrodeposition of gold nanoparticles from ionic liquid microemulsion," *Colloid and Polymer Science*, vol. 288, no. 10-11, pp. 1097–1103, 2010.

[15] M. M. Rahman, A. J. S. Ahammad, J. H. Jin, S. J. Ahn, and J. J. Lee, "A comprehensive review of glucose biosensors based on nanostructured metal-oxides," *Sensors*, vol. 10, no. 5, pp. 4855–4886, 2010.

[16] X. Ji, K. T. Lee, R. Holden et al., "Nanocrystalline intermetallics on mesoporous carbon for direct formic acid fuel cell anodes," *Nature Chemistry*, vol. 2, no. 4, pp. 286–293, 2010.

[17] J. S. Spendelow, P. K. Babu, and A. Wieckowski, "Electrocatalytic oxidation of carbon monoxide and methanol on platinum surfaces decorated with ruthenium," *Current Opinion in Solid State and Materials Science*, vol. 9, no. 1-2, pp. 37–48, 2005.

[18] S. Alayoglu, A. U. Nilekar, M. Mavrikakis, and B. Eichhorn, "Ru-Pt core-shell nanoparticles for preferential oxidation of carbon monoxide in hydrogen," *Nature Materials*, vol. 7, no. 4, pp. 333–338, 2008.

[19] F. Xiao, F. Zhao, Y. Zhang, G. Guo, and B. Zeng, "Ultrasonic electrodeposition of gold—platinum alloy nanoparticles on ionic liquid—chitosan composite film and their application in fabricating nonenzyme hydrogen peroxide sensors," *Journal of Physical Chemistry C*, vol. 113, no. 3, pp. 849–855, 2009.

[20] D. N. Muraviev, J. Macanás, P. Ruiz, and M. Munoz, "Synthesis, stability and electrocatalytic activity of polymer-stabilized monometallic Pt and bimetallic Pt/Cu core-shell nanoparticles," *Physica Status Solidi A*, vol. 205, no. 6, pp. 1460–1464, 2008.

[21] M. Rajkumar, S. Thiagarajan, and S.-M. Chen, "Electrochemical fabrication of Rh-Pd particles and electrocatalytic applications," *Journal of Applied Electrochemistry*, vol. 41, no. 6, pp. 663–668, 2011.

[22] A. Radoi, D. Compagnone, E. Devic, and G. Palleschi, "Low potential detection of NADH with Prussian Blue bulk modified screen-printed electrodes and recombinant NADH oxidase from Thermus thermophilus," *Sensors and Actuators B*, vol. 121, no. 2, pp. 501–506, 2007.

[23] L. Deng, Y. Wang, L. Shang, D. Wen, F. Wang, and S. Dong, "A sensitive NADH and glucose biosensor tuned by visible light based on thionine bridged carbon nanotubes and gold nanoparticles multilayer," *Biosensors and Bioelectronics*, vol. 24, no. 4, pp. 951–957, 2008.

[24] A. L. Sanford, S. W. Morton, K. L. Whitehouse et al., "Voltammetric detection of hydrogen peroxide at carbon fiber microelectrodes," *Analytical Chemistry*, vol. 82, no. 12, pp. 5205–5210, 2010.

[25] C. J. Hsueh, J. H. Wang, L. M. Dai, and C. C. Liu, "Determination of alanine aminotransferase with an electrochemical nano Ir-C biosensor for the screening of liver diseases," *Biosensor*, vol. 1, no. 3, pp. 107–117, 2011.

[26] J. R. Windmiller, N. Zhou, M.-C. Chuang et al., "Microneedle array-based carbon paste amperometric sensors and biosensors," *Analyst*, vol. 136, no. 9, pp. 1846–1851, 2011.

[27] D. Wang, Q. Peng, and Y. Li, "Nanocrystalline intermetallics and alloys," *Nano Research*, vol. 3, no. 8, pp. 574–580, 2010.

[28] S. Chen, R. Yuan, Y. Chai, L. Zhang, N. Wang, and X. Li, "Amperometric third-generation hydrogen peroxide biosensor based on the immobilization of hemoglobin on multiwall carbon nanotubes and gold colloidal nanoparticles," *Biosensors and Bioelectronics*, vol. 22, no. 7, pp. 1268–1274, 2007.

[29] W. Lu, G. Chang, Y. Luo, F. Liao, and X. Sun, "Method for effective immobilization of Ag nanoparticles/graphene oxide composites on single-stranded DNA modified gold electrode for enzymeless H_2O_2 detection," *Journal of Materials Science*, vol. 46, no. 15, pp. 5260–5266, 2011.

[30] X. Cui, Z. Li, Y. Yang, W. Zhang, and Q. Wang, "Low-potential sensitive hydrogen peroxide detection based on nanotubular TiO_2 and platinum composite electrode," *Electroanalysis*, vol. 20, no. 9, pp. 970–975, 2008.

[31] S. Hrapovic, Y. Liu, K. B. Male, and J. H. T. Luong, "Electrochemical biosensing platforms using platinum nanoparticles and carbon nanotubes," *Analytical Chemistry*, vol. 76, no. 4, pp. 1083–1088, 2004.

[32] S. A. G. Evans, J. M. Elliott, L. M. Andrews, P. N. Bartlett, P. J. Doyle, and G. Denuault, "Detection of hydrogen peroxide at mesoporous platinum microelectrodes," *Analytical Chemistry*, vol. 74, no. 6, pp. 1322–1326, 2002.